Research Journal of Engineering Sciences ____ ISSN 2278 – 9472
Vol. **4(4),** 1-8, April **(2015)** *Res. J. Engineering Sci.*

Nonlinear Buckling Analysis of Laminated Composite Twisted Plate

S. Prashanth[1], Indrajeeth M.S.[2] and A.V. Asha[2]
[1]Department of Civil Engineering, Raghu Institute Technology, Visakhapatnam-531162, INDIA
[2]Department of Civil Engineering, National Institute of Technology, Rourkela-769008, INDIA

Available online at: www.isca.in, www.isca.me
Received 11th November 2014, revised 11th February 2015, accepted 20th April 2015

Abstract

The twisted plate has various applications in turbine blades, compressor blades, fan blades and particularly in gas turbines. Many of these plates are subjected to in-plane load due to fluid or aerodynamic pressures. Buckling of such plates is of special importance especially if the plates are thin. Hence it is necessary to study their behaviour under different types of loads.. For a complete buckling study, a geometrically nonlinear analysis should be carried out. In a geometrically nonlinear analysis, the stiffness matrix of the structure is updated between loading increments to take into account deformations which affect the structural behaviour unlike a linear buckling analysis where the stiffness matrix is constant through the analysis. .The buckling of twisted plates is investigated by a nonlinear analysis. The effect of number of layers, changing angle of twist, width to thickness ratio, aspect ratio, etc are studied. It is observed in all cases that the buckling load by nonlinear analysis is lesser than that predicted by a linear analysis which proves the importance of the present study.

Keywords: Buckling, NonLinear Buckling analysis, Geometric Nonlinearity, Ansys, pretwist.

Introduction

Laminated composite plates have increasing applications due to their high stiffness and strength-to-weight ratios, high fatigue life, resistance to corrosion and other properties of composites. The plates are often subjected to axial periodic forces due to axial components of aerodynamic or hydrodynamic forces acting on it. These can be designed through the variation of fibre orientation and stacking sequence to obtain an efficient design**.** For a complete buckling study, a geometrically nonlinear analysis should be carried out. Nonlinearity due to material and boundary conditions can also be investigated if required. Material nonlinearity during buckling is due to yielding or boundary nonlinearity. Modelling of nonlinear effects should be done in such a way so as to assess the results of additional modelling at every stage. This helps to understand the structural behaviour. A nonlinear analysis calculates actual displacements and stresses as opposed to linear buckling analysis, which only calculates the potential buckling shape. A nonlinear analysis is required when the stiffness of the structure changes due to the deformation of the structure. In a nonlinear analysis, the stiffness does not remain same. It has to be changed with changing geometry or material property. If the change in stiffness is only due to change in shape, then the nonlinear behaviour is defined as geometric nonlinearity. If it is due to changing material property, then the nonlinear behaviour is defined as material nonlinearity. A linear buckling analysis can be applied to compute the Euler buckling load, i.e., the load under which a structure will buckle. Assumptions used in the FEA model may result in the predicted buckling load being much higher in the FEA model than for the actual structure. The results of the linear buckling analysis should be used carefully. A nonlinear buckling analysis of a structure, thus helps to understand the results in a better way.

A large amount of research has been devoted to the analysis of vibration, buckling and post buckling behaviour, failure and so on of such structures. Bauer and Reiss studied the nonlinear deflections of a thin elastic simply-supported rectangular plate[1]. They proved that the plate cannot buckle for thrusts less than or equal to the lowest eigenvalue of the linearized buckling problem. Crispino and Benson studied the stability of thin, rectangular, orthotropic plates which were in a state of tension and twist[2]. A computational model for buckling and post buckling analysis of stiffened panels was developed by Byklum and Amdhal which provided accurate results for use in design of ships and offshore structures[3]. Nonlinear buckling analysis of shear deformable plates was studied by Purbolaksono and Aliabadi[4]. Shaikh Akhlaque-E-Rasul and Ganesan developed a simplified methodology to predict the stability limit load that required only two load steps[5]. Lee determined the critical buckling pressure of a submarine using Finite Element Analysis (FEA)[6]. Sofiyev et al examined the buckling behaviour of cross-ply laminated non-homogeneous orthotropic truncated conical shells under a uniform axial load [7]. Alinia et al investigated the inelastic buckling behavior of thick plates under interactive shear and in-plane bending[8]. Buckling of a cantilever plate uniformly loaded in its plane was studied by Lachut and Sader[9]. The nonlinear buckling and post-buckling behaviour of functionally graded stiffened thin circular cylindrical shells subjected to external pressure were investigated by Dao Van Dung and Le Kha Hoa[10]. Dao HuyBich et al presented an analytical approach to investigate the nonlinear static and dynamic buckling of imperfect eccentrically stiffened functionally graded thin circular cylindrical shells subjected to axial compression[11]. Yuan and Wang studied the non-linear buckling analysis of inclined circular cylinder-in-cylinder by the discrete singular convolution[12]. Shariyat investigated dynamic buckling of imperfect sandwich plates subjected to thermo-mechanical loads[13]. Danial Panahandeh-Shahraki et al analysed laminated composite cylindrical panels resting on tensionless foundation under axial compression[14]. Using higher order shear deformation theory, buckling of composite plate assemblies was studied by F.A. Fazzolari et al[15].

The laminated composite panels are primarily used in shipbuilding, aerospace and in engineering constructions as well. These structures are highly sensitive to geometrical and mechanical imperfections. The defects include different directions of fibre, variations in thickness, delamination or initial deformations. Plates in a ship structure are subjected to any combination of in plane, out of plane and shear loads[6]. Due to the geometry and nature of loading of the ship hull, buckling is one of the most important failure criteria of these structures.

The twisted cantilever panels have significant applications in turbine blades, compressor blades, fan blades, aircraft or marine propellers, chopper blades, and predominantly in gas turbines. Today twisted plates are key structural units in the research field. Because of the use of twisted plates in turbo-machinery, aeronautical and aerospace industries and so on, it is mandatory to understand both the buckling and vibration characteristics of the twisted plates. The twisted plates are also subjected to loads due to fluid pressure or transverse loads[16].

Methodology

For complex geometrical and boundary conditions, analytical method are not so easily adaptable, so numerical methods like finite element method have been used[15]. The finite element formulation is developed here by for the structural analysis of composite twisted shell panels using first order shear deformation theory. ANSYS software which is a finite element software has been used for the study.

The hardness of a structure changes due to the change in shape of the construction during its deformation under loads or due to material property changing due to large distortions. If the deformation is small, and so it may be taken for granted that the configuration or material property does not change, that is the initial stiffness of the structure does not vary with the deformed configuration[17]. This is the fundamental assumption in a linear analysis.

The plate is made up with bonded layers, where each lamina is considered to be homogenous and orthotropic and made of unidirectional fiber-reinforced material. The orthotropic axes of symmetry in each lamina are oriented at an arbitrary angle to plate axes. The present study mainly aims to analyse the laminated composite twisted plates under the in plane loading conditions shown in figure-1. Methodology involves the linear buckling and nonlinear buckling analysis of twisted plates. The present work consists of developing FEA models of a laminated composite twisted plate under an in plane load.

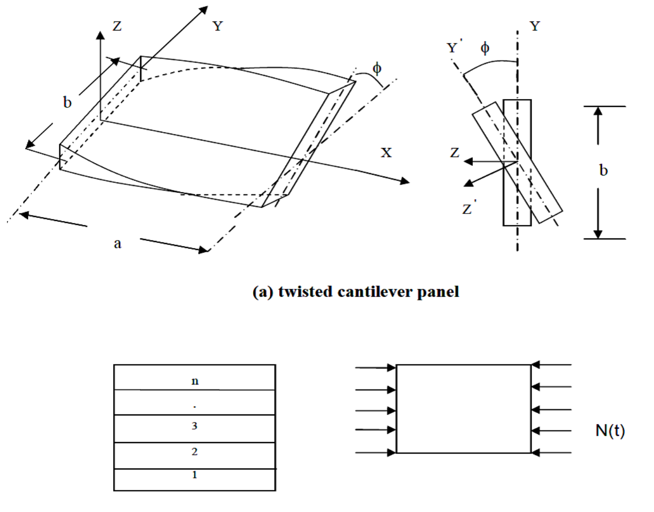

(a) twisted cantilever panel

(b) the lamination (c) planform subjected to in-plane load

Figure-1
Laminated composite twisted panel with in-plane loads

Formulations: Governing Differential Equations: The governing differential equations of equilibrium of a shear deformable doubly curved pretwisted panel subjected to external in-plane loading can be expressed as[17,18].

$$\frac{\partial N_x}{\partial x}+\frac{\partial N_{xy}}{\partial y}-\frac{1}{2}\left(\frac{1}{R_y}-\frac{1}{R_x}\right)\frac{\partial M_{xy}}{\partial y}+\frac{Q_x}{R_x}+\frac{Q_y}{R_{xy}} = P_1\frac{\partial^2 u}{\partial t^2}+P_2\frac{\partial^2 \theta_x}{\partial t^2}$$

$$\frac{\partial N_{xy}}{\partial x}+\frac{\partial N_y}{\partial y}+\frac{1}{2}\left(\frac{1}{R_y}-\frac{1}{R_x}\right)\frac{\partial M_{xy}}{\partial x}+\frac{Q_y}{R_y}+\frac{Q_x}{R_{xy}} = P_1\frac{\partial^2 v}{\partial t^2}+P_2\frac{\partial^2 \theta_y}{\partial t^2}$$

$$\frac{\partial Q_x}{\partial x}+\frac{\partial Q_y}{\partial y}-\frac{N_x}{R_x}-\frac{N_x}{R_y}-2\frac{N_{xy}}{R_{xy}}+N_x^0\frac{\partial^2 w}{\partial x^2}+N_y^0\frac{\partial^2 w}{\partial y^2} = P_1\frac{\partial^2 w}{\partial t^2}$$

$$\frac{\partial M_x}{\partial x}+\frac{\partial M_{xy}}{\partial y}-Q_x = P_1\frac{\partial^2 \theta_x}{\partial t^2}+P_2\frac{\partial^2 u}{\partial t^2}$$

$$\frac{\partial M_{xy}}{\partial x}+\frac{\partial M_y}{\partial y}-Q_y = P_1\frac{\partial^2 \theta_y}{\partial t^2}+P_2\frac{\partial^2 v}{\partial t^2} \quad (1)$$

Also N_x^0 and N_y^0 are the external loading in the X and Y direction respectively. The constants R_x, R_y and R_{xy} are the radii of curvature in the x and y directions and the radius of twist.

$$(P_1, P_2, P_3) = \sum_{k=1}^{n}\int_{Z_{k-1}}^{Z_k}(\rho)_k(1, z, z^2)dz \quad (2)$$

Where: n= number of layers of the laminated composite twisted curved panel and $(\rho)_k$ = mass density of k_{th} layer from the mid-plane.

First order shear deformation theory is used and the displacement field assumes that the mid –plane normal remains straight before and after deformation, but not necessarily normal after deformation, so that

$$u(x,y,z)= u_0(x,y)+ z\,\theta_y(x,y)$$
$$v(x,y,z)= u_0(x,y)+ z\,\theta_x(x,y) \quad (3)$$
$$w(x,y,z)= w_0(x,y)$$

Where *u, v, w* and u_0, v_0, w_0 are displacement in the *x, y, z* directions at any point and at the mid surface respectively $\theta_x and\ \theta_y$ and are the rotations of the midsurface normal about the x and y axes respectively.

Strain Displacement Relations: Green-Lagrange's strain displacement relations are used throughout. The linear strain displacement relations for a twisted shell element are:

$$\xi_{xl}=\frac{\partial u}{\partial x}+\frac{w}{R_x}+zk_x$$
$$\xi_{yl}=\frac{\partial v}{\partial y}+\frac{w}{R_y}+zk_y$$
$$\gamma_{xyl}=\frac{\partial u}{\partial y}+\frac{\partial v}{\partial x}+\frac{2w}{R_{xy}}+zk_{xy} \quad (4)$$
$$\gamma_{xzl}=\frac{\partial w}{\partial x}+\theta_x-\frac{u}{R_x}-\frac{v}{R_{xy}}$$
$$\gamma_{yzl}=\frac{\partial w}{\partial y}+\theta_y-\frac{v}{R_y}-\frac{u}{R_{xy}}$$

Where the bending strains are expressed as

$$k_x=\frac{\partial\theta_x}{\partial x},\ k_y=\frac{\partial\theta_y}{\partial y}$$
$$k_{xy}=\frac{\partial\theta_x}{\partial y}+\frac{\partial\theta_y}{\partial x}+\frac{1}{2}\left(\frac{1}{R_y}-\frac{1}{R_x}\right)\left(\frac{\partial v}{\partial x}-\frac{\partial u}{\partial y}\right) \quad (5)$$

The linear strains can be expresses in term of displacements as:

$$\{\varepsilon\}=[B]\ \{d_e\} \quad (6)$$

$$\text{Where,}\{d_e\}=\{u_1v_1w_1\theta_{x1}\theta_{y1}\ \ldots .\ u_8v_8w_8\theta_{x8}\theta_{y8}\} \quad (7)$$

$$[B]=[[B_1],[B_2]..\ \ldots\ldots\ldots\ldots\ldots\ldots.[B_8]] \quad (8)$$

$$[B_i]=\begin{bmatrix} N_{i,}x & 0 & \frac{N_i}{R_x} & 0 & 0 \\ 0 & N_{i,}y & \frac{N_i}{R_y} & 0 & 0 \\ N_{i,}y & N_{i,}x & 2\frac{N_i}{R_{xy}} & 0 & 0 \\ 0 & 0 & 0 & N_{i,}x & 0 \\ 0 & 0 & 0 & 0 & N_{i,}y \\ 0 & 0 & 0 & N_{i,}y & N_{i,}x \\ 0 & 0 & N_{i,}x & N_i & 0 \\ 0 & 0 & N_{i,}y & 0 & N_i \end{bmatrix} \quad (9)$$

Constitutive Relations: The basic composite twisted curved panel is considered to be composed of composite material laminates (typically thin layers). The material of each lamina consists of parallel, continuous fibers (e.g. graphite, boron, glass) of one material embedded in a matrix material (e.g. epoxy resin). Each layer may be regarded on a macroscopic scale as being homogeneous and orthotropic. The laminated fiber reinforced shell is assumed to consist of a number of thin laminates as shown in figure-3. The principle material axes are indicated by 1 and 2 and moduli of elasticity of a lamina along these directions are E_{11} and E_{22} respectively. For the plane stress state,$\sigma_{0=0}$

$$\begin{bmatrix}\sigma_x\\ \sigma_y\\ \tau_{xy}\\ \tau_{xz}\\ \tau_{yz}\end{bmatrix}=\begin{bmatrix} Q_{11} & Q_{12} & 0 & 0 & 0\\ Q_{12} & Q_{22} & 0 & 0 & 0\\ 0 & 0 & Q_{66} & 0 & 0\\ 0 & 0 & 0 & Q_{44} & 0\\ 0 & 0 & 0 & 0 & Q_{55}\end{bmatrix}\begin{bmatrix}\varepsilon_x\\ \varepsilon_y\\ \gamma_{xy}\\ \gamma_{xz}\\ \gamma_{yz}\end{bmatrix} \quad (10)$$

$$\text{Where } Q_{11}=\frac{E_{11}}{(1-v_{12}v_{21})} \qquad Q_{12}=\frac{E_{11}v_{21}}{(1-v_{12}v_{21})}$$
$$Q_{21}=\frac{v_{12}E_{22}}{(1-v_{12}v_{21})} \qquad Q_{22}=\frac{E_{22}}{(1-v_{12}v_{21})} \quad (11)$$
$$Q_{66}=G_{12} \qquad Q_{44}=\mathrm{k}G_{13}$$
$$Q_{55}=kG_{23}$$

The on –axis elastic constant matrix corresponding to the fiber direction is given by

$$[Q_{ij}]=\begin{bmatrix} Q_{11} & Q_{12} & 0 & 0 & 0\\ Q_{12} & Q_{22} & 0 & 0 & 0\\ 0 & 0 & Q_{66} & 0 & 0\\ 0 & 0 & 0 & Q_{44} & 0\\ 0 & 0 & 0 & 0 & Q_{55}\end{bmatrix} \quad (12)$$

If the major and minor Poisson's ratio are ν_{12} and ν_{21}, then using reciprocal relation one obtains the following well known expression

$$\frac{\vartheta_{12}}{E_{11}}=\frac{\vartheta_{21}}{E_{22}} \quad (13)$$

Standard coordinate transformation is required to obtain the elastic constant matrix for any arbitrary principle axes with which the material principal axes makes an angle θ. Thus the off-axis elastic constant matrix is obtained from the on-axis elastic constant matrix as.

$$[\bar{Q}_{ij}]=\begin{bmatrix} \bar{Q}_{11} & \bar{Q}_{12} & \bar{Q}_{16} & 0 & 0\\ \bar{Q}_{12} & \bar{Q}_{22} & \bar{Q}_{26} & 0 & 0\\ \bar{Q}_{16} & \bar{Q}_{26} & \bar{Q}_{66} & 0 & 0\\ 0 & 0 & 0 & \bar{Q}_{44} & \bar{Q}_{45}\\ 0 & 0 & 0 & \bar{Q}_{45} & \bar{Q}_{55}\end{bmatrix} \quad (14)$$

$$[\bar{Q}_{ij}]=[T]^T][Q_{ij}][T] \quad (15)$$

Where:T is transformation matrix. After transformation the elastic stiffness coefficients are:

$$\bar{Q}_{11}=Q_{11}m^4+2(Q_{12}+2Q_{66})m^2n^2+Q_{22}n^4$$
$$\bar{Q}_{12}=(Q_{11}+Q_{22}-4Q_{66})m^2n^2+Q_{12}(m^4+n^4)$$
$$\bar{Q}_{22}=Q_{11}n^4+2(Q_{12}+Q_{66})m^2n^2+Q_{22}m^4 \quad (16)$$
$$\bar{Q}_{16}=(Q_{11}-Q_{12}-2Q_{66})nm^3+(Q_{12}-Q_{22}+2Q_{66})n^3m$$
$$\bar{Q}_{26}=(Q_{11}-Q_{12}-2Q_{66})mn^3+(Q_{12}-Q_{22}+2Q_{66})m^3n$$
$$\bar{Q}_{66}=(Q_{11}+Q_{22}-2Q_{12}-2Q_{66})n^2m^2+Q_{66}(n^4+m^4)$$

The elastic constant matrix corresponding to transverse shear deformation is

$$\bar{Q}_{44} = G_{13}m^2 + G_{23}n^2$$
$$\bar{Q}_{45} = (G_{13} - G_{23})mn \quad (17)$$
$$\bar{Q}_{55} = G_{13}n^2 + G_{23}m^2$$

Where: m = cosθ and n = sinθ

The stress strain relations are

$$\begin{bmatrix} \sigma_x \\ \sigma_y \\ \tau_{xy} \\ \tau_{xz} \\ \tau_{yz} \end{bmatrix} = \begin{bmatrix} \bar{Q}_{11} & \bar{Q}_{12} & \bar{Q}_{16} & 0 & 0 \\ \bar{Q}_{12} & \bar{Q}_{22} & \bar{Q}_{26} & 0 & 0 \\ \bar{Q}_{16} & \bar{Q}_{26} & \bar{Q}_{66} & 0 & 0 \\ 0 & 0 & 0 & \bar{Q}_{44} & \bar{Q}_{45} \\ 0 & 0 & 0 & \bar{Q}_{45} & \bar{Q}_{55} \end{bmatrix} \begin{bmatrix} \varepsilon_x \\ \varepsilon_y \\ \gamma_{xy} \\ \gamma_{xz} \\ \gamma_{yz} \end{bmatrix} \quad (18)$$

The forces and moment resultants are obtained by integration through the thickness h for stresses as

$$\begin{bmatrix} N_x \\ N_y \\ N_{xy} \\ M_x \\ M_Y \\ M_{xY} \\ Q_x \\ Q_Y \end{bmatrix} = \int_{-h/2}^{h/2} \begin{Bmatrix} \sigma_x \\ \sigma_x \\ \tau_{xy} \\ \sigma_x z \\ \sigma_{yz} \\ \tau_{xy} z \\ \tau_{xz} \\ \tau_{yz} \end{Bmatrix} dz \quad (19)$$

Where: σ_x, σ_y are the normal stresses along X and Y directionτ_{xy}, τ_{xz} and τ_{yz} are shear stresses in xy, xz and yz planes respectively.

Considering only in-plane deformation, the constitutive relation for the initial plane stress analysis is

$$\begin{Bmatrix} N_x \\ N_y \\ N_{xy} \end{Bmatrix} = \begin{bmatrix} A_{11} & A_{12} & A_{16} \\ A_{21} & A_{22} & A_{26} \\ A_{31} & A_{32} & A_{66} \end{bmatrix} \begin{Bmatrix} \varepsilon_x \\ \varepsilon_y \\ \gamma_{xy} \end{Bmatrix} \quad (20)$$

The extensional stiffness for an isotropic material with material properties E and v are

$$[D_P] = \begin{bmatrix} \frac{Eh}{1-v^2} & \frac{Eh}{1-v^2} & 0 \\ \frac{vEh}{1-v^2} & \frac{Eh}{1-v^2} & 0 \\ 0 & 0 & \frac{Eh}{2(1+v)} \end{bmatrix} \quad (21)$$

The constitutive relationships for bending transverse shear of a doubly curved shell becomes

$$\begin{Bmatrix} N_x \\ N_P \\ N_{xy} \\ M_x \\ M_y \\ M_{xy} \\ Q_x \\ Q_y \end{Bmatrix} \begin{bmatrix} A_{11} & A_{12} & A_{16} & B_{11} & B_{112} & B_{16} & 0 & 0 \\ A_{21} & A_{22} & A_{26} & B_{12} & B_{22} & B_{26} & 0 & 0 \\ A_{16} & A_{26} & A_{66} & B_{11} & B_{12} & B_{16} & 0 & 0 \\ B_{11} & B_{12} & B_{16} & D_{11} & D_{12} & D_{16} & 0 & 0 \\ B_{12} & B_{22} & B_{26} & D_{12} & D_{22} & D_{26} & 0 & 0 \\ B_{16} & B_{26} & B_{66} & D_{16} & D_{26} & D_{66} & 0 & 0 \\ 0 & 0 & 0 & 0 & 0 & 0 & S_{44} & S_{45} \\ 0 & 0 & 0 & 0 & 0 & 0 & S_{45} & S_{55} \end{bmatrix} \begin{Bmatrix} \varepsilon_x \\ \varepsilon_y \\ \gamma_{xy} \\ k_x \\ k_y \\ k_{xy} \\ \gamma_{xz} \\ \gamma_{yz} \end{Bmatrix} \quad (22)$$

This can also be stated as $\begin{Bmatrix} N_i \\ M_i \\ Q_i \end{Bmatrix} = \begin{bmatrix} A_{ij} & B_{ij} & 0 \\ B_{ij} & D_{ij} & 0 \\ 0 & 0 & S_{ij} \end{bmatrix} \begin{Bmatrix} \varepsilon_j \\ k_j \\ \gamma_m \end{Bmatrix}$ (23)

$$\{F\} = [D]\{\varepsilon\} \quad (24)$$

Where A_{ij}, B_{ij}, $D_{ij}$and S_{ij} are the extensional, bending-stretching coupling, bending and transverse shear stiffness. They may be defined as:

$$A_{ij} = \sum_{k=1}^{n} \overline{(Q_{ij})}_k (z_k - z_{k-1})$$
$$B_{ij} = \frac{1}{2} \sum_{k=1}^{n} \overline{(Q_{ij})}_k (z_k^2 - z_{k-1}^2)$$
$$D_{ij} = \frac{1}{3} \sum_{k=1}^{n} \overline{(Q_{ij})}_k (z_k^3 - z_{k-1}^3)\,; i,j = 1,2,6 \quad (25)$$
$$S_{ij} = k \sum_{k=1}^{n} \overline{(Q_{ij})}_k (z_k - z_{k-1})\,; i,j = 4,5$$

And k is the transverse shear correction factor. The accurate prediction for anisotropic laminates depends on a number of laminate properties and is also problem dependent. A shear correction factor of5/6 is used in the present formulation or all numerical computations.

Derivation of element matrices: The element matrices in natural coordinate system are deriver as:

Element plane elastic stiffness matrix

$$[k_P] = \int_{-1}^{1}\int_{-1}^{1} [B_P]^T [D_P][B_P]|J|\,d\xi d\eta \quad (30)$$

Element elastic stiffness matrix

$$[k_e] = \int_{-1}^{1}\int_{-1}^{1} [B]^T [D][B]|J|\,d\xi d\eta \quad (31)$$

Where the shape function matrix

$$[N] = \begin{bmatrix} N_i & 0 & 0 & 0 & 0 \\ 0 & N_i & 0 & 0 & 0 \\ 0 & 0 & N_i & 0 & 0 \\ 0 & 0 & 0 & N_i & 0 \\ 0 & 0 & 0 & 0 & N_i \end{bmatrix} \text{i=1, 2…..8} \quad (32)$$

Where: [B],[D],[N] are the strain-displacement matrix stress-strain and shape function matrix and $|J|$ is the Jacobian determinant.

Geometric stiffness matrix: The element geometric stiffness matrix for the twisted shell is derived using the non-linear in-plane Green's strains with curvature component using the procedure explained by Cook, Malkus and Plesha[20]. The geometric stiffness matrix is a function of in-plane stress distribution in the element due to applied edge loading. Plane stress analysis is carried out using the finite element technique to determine the stresses and these are used to formulate the geometric stiffness matrices.

$$U_2 = \int_V [\sigma^0]^T \{\varepsilon_{nl}\} dV \quad (33)$$

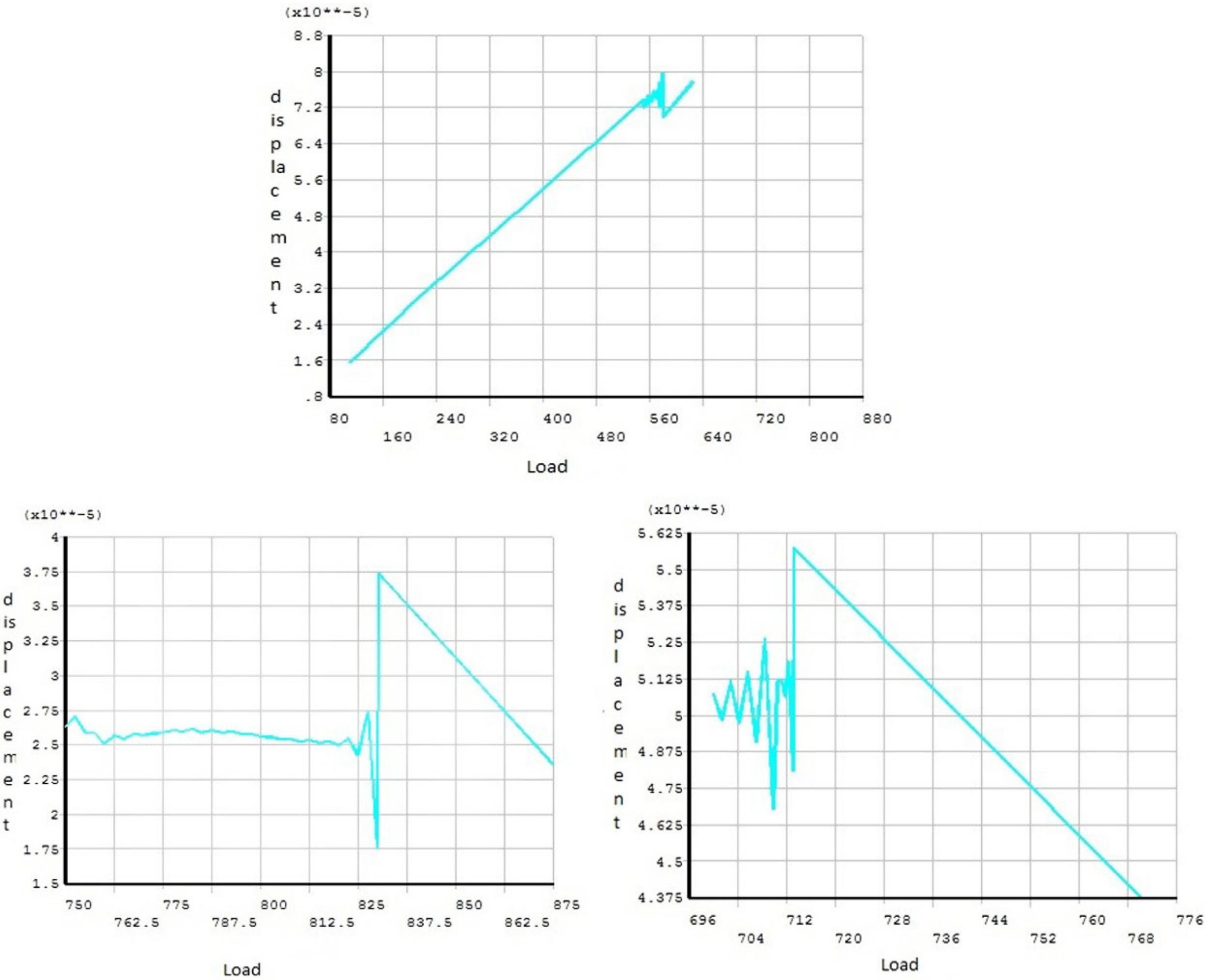

Figure-2
Displacement vs Load for a Cantilever plate with different Angle of Twist for a non-linear analysis

The non-linear strain components are as follow:

$$\varepsilon_{xnl} = \frac{1}{2}\left(\frac{\partial u}{\partial x}\right)^2 + \frac{1}{2}\left(\frac{\partial v}{\partial x}\right)^2 - \frac{1}{2}\left(\frac{\partial w}{\partial x} - \frac{u}{R_x}\right)^2 + \frac{1}{2}z^2\left[\left(\frac{\partial \theta_x}{\partial x}\right)^2 + \left(\frac{\partial \theta_y}{\partial x}\right)^2\right] \tag{34}$$

$$\varepsilon_{ynl} = \frac{1}{2}\left(\frac{\partial u}{\partial y}\right)^2 + \frac{1}{2}\left(\frac{\partial v}{\partial y}\right)^2 - \frac{1}{2}\left(\frac{\partial w}{\partial y} - \frac{u}{R_y}\right)^2 + \frac{1}{2}z^2\left[\left(\frac{\partial \theta_x}{\partial y}\right)^2 + \left(\frac{\partial \theta_y}{\partial y}\right)^2\right]$$

$$\gamma_{xnl} = \frac{\partial u}{\partial x}\left(\frac{\partial u}{\partial y}\right) + \frac{\partial v}{\partial x}\left(\frac{\partial v}{\partial y}\right) + \left(\frac{\partial w}{\partial x} - \frac{u}{R_x}\right)\left(\frac{\partial w}{\partial y} - \frac{v}{R_y}\right) + z^2\left[\left(\frac{\partial \theta_x}{\partial x}\right)\left(\frac{\partial \theta_x}{\partial y}\right) + \left(\frac{\partial \theta_y}{\partial x}\right)\left(\frac{\partial \theta_y}{\partial y}\right)\right]$$

Using the non-linear strains, the strain energy can be written as

$$U_2 = \int_A \frac{h}{2}\left[\sigma_x^0\left\{\left(\frac{\partial u}{\partial y}\right)^2 + \left(\frac{\partial u}{\partial y}\right)^2 + \left(\frac{\partial w}{\partial y} - \frac{u}{R_y}\right)^2\right\} + \sigma_y^0\left\{\left(\frac{\partial u}{\partial y}\right)^2 + \left(\frac{\partial u}{\partial y}\right)^2 + \left(\frac{\partial w}{\partial y} - \frac{u}{R_y}\right)^2\right\} + 2\tau_{xy}^0\left\{\left(\frac{\partial u}{\partial y}\frac{\partial u}{\partial y}\right) + \left(\frac{\partial v}{\partial y}\frac{\partial v}{\partial y}\right) + \left(\frac{\partial w}{\partial y} - \frac{u}{R_y}\right)\left(\frac{\partial w}{\partial y} - \frac{u}{R_y}\right)\right\}\right] \int_A \frac{h^2}{24}\left[\sigma_x^0\left\{\left(\frac{\partial \theta_x}{\partial x}\right)^2 + \left(\frac{\partial \theta_y}{\partial x}\right)^2 + \right\} + \sigma_y^0\left\{\left(\frac{\partial \theta_y}{\partial y}\right)^2 + \left(\frac{\partial \theta_x}{\partial y}\right)^2\right\} + 2\tau_{xy}^0\left\{\left(\frac{\partial \theta_y}{\partial x}\frac{\partial \theta_x}{\partial y}\right) + \left(\frac{\partial \theta_x}{\partial x}\frac{\partial \theta_y}{\partial y}\right)\right\}\right] \tag{35}$$

This can also be written as

$$U_2 = \frac{1}{2}\int_v [f]^r [S][f]\, dV \tag{36}$$

Where

$$\{f\} = \left[\frac{\partial u}{\partial x}, \frac{\partial u}{\partial y}, \frac{\partial v}{\partial x}, \frac{\partial v}{\partial y}, \left(\frac{\partial w}{\partial x} - \frac{u}{R_x}\right), \left(\frac{\partial w}{\partial y} - \frac{v}{R_y}\right), \frac{\partial \theta_x}{\partial x}, \frac{\partial \theta_x}{\partial y}, \frac{\partial \theta_y}{\partial x}, \frac{\partial \theta_y}{\partial y}\right]^r \quad (37)$$

And

$$[S] = \begin{bmatrix} [s] & 0 & 0 & 0 & 0 \\ 0 & [s] & 0 & 0 & 0 \\ 0 & 0 & [s] & 0 & 0 \\ 0 & 0 & 0 & [s] & 0 \\ 0 & 0 & 0 & 0 & [s] \end{bmatrix} \quad (38)$$

Where

$$[s] = \begin{bmatrix} \sigma_x^0 & \tau_{xy}^0 \\ \tau_{xy}^0 & \sigma_y^0 \end{bmatrix} = \frac{1}{h}\begin{bmatrix} N_x^0 & N_{xy}^0 \\ N_{xy}^0 & N_y^0 \end{bmatrix} \quad (39)$$

The in-plane stress resultants $N_x^0, N_x^0$and N_x^0 at each Gauss point are obtained separately by plane stress analysis and the geometric stiffness matrix is formed for these stress resultants

$$\{f\} = [G]\{q_e\} \quad (40)$$

Where

$$\{q_e\} = [u\ v\ w\ \theta_x \theta_x]^T \quad (41)$$

The strain energy becomes

$$U_2 = \frac{1}{2}[q]^r[G]^T[S][G]\{q\}dV = \frac{1}{2}\{q_e\}^T[K_e]_e[q_e] \quad (42)$$

Where the element geometric stiffness matrix

$$[K_e]_e = \int_{-1}^{1}\int_{-1}^{1}[G]^T[S][G]|J|d\xi d\eta \quad (43)$$

$$[G] = \begin{bmatrix} N_{i,}x & 0 & 0 & 0 & 0 \\ N_{i,}y & 0 & 0 & 0 & 0 \\ 0 & N_{i,}x & 0 & 0 & 0 \\ 0 & N_{i,}y & 0 & 0 & 0 \\ 0 & 0 & N_{i,}x & 0 & 0 \\ 0 & 0 & N_{i,}y & 0 & 0 \\ 0 & 0 & 0 & N_{i,}x & 0 \\ 0 & 0 & 0 & N_{i,}y & 0 \\ 0 & 0 & 0 & 0 & N_{i,}x \\ 0 & 0 & 0 & 0 & N_{i,}y \end{bmatrix} \quad (44)$$

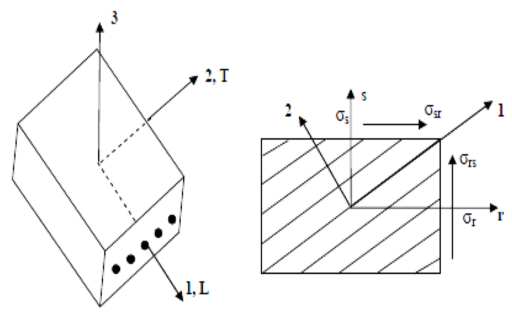

Figure-3
Laminated shell element showing principal axes and laminate directions

Results and Discussion

Nonlinear buckling analysis is a static analysis through which we can incorporate the nonlinearities due to loading, supports and end conditions. Here we consider the geometric nonlinearity only for our study. After analysing the plate for linear analysis we have to proceed for nonlinear analysis. We have to give a deformation by applying a small load at the point of maximum displacement obtained from linear buckling analysis. After giving a deformation we will get our analysis done with a geometric nonlinearity. The load will start decreasing after the solver extracts two number of modes, the load goes on decreasing and then it will increase a little and continue to be constant. The load at which it starts increasing is the buckling load from nonlinear analysis which is less than the buckling load obtained from linear buckling. A graph is plotted between displacement and load at the node which was given deformation initially. This graph gives the buckling value.

Convergence study and validation of results: The convergence study is first done for square isotropic plates clamped on all the edges for different mesh divisions and is shown in table-1. Based on this study, a 12 x 12 mesh was chosen for solving the problem.

Table-1
Convergence study of Non-dimensional buckling load (λ) of square isotropic plate a/b=1, h = 1mm, E = 210GPa, ν= 0.3, $\lambda=N_xb^2/E_{22}h^3$

Mesh division	Buckling load (kN/m)	Non-dimensional Buckling load
6 x 6	204.10	10.200
8 x 8	200.30	10.015
10 x 10	199.72	9.986
12 x 12	199.65	9.983
Sandeep Sing et al[19]		9.96

Variation of buckling load with aspect ratio for a/h of 100 with different ply lay-ups simply supported on all edges shown in table-2. From table-2 it can be seen that the buckling load increases as the number of layers increases and as the aspect ratio increases, i.e., the buckling load is high for rectangular plates than square plates. Also it can be observed that the symmetrical arrangement of 4 layer ply has more buckling value than the 8 layer asymmetrical ply.

Also in all cases the non-linear buckling load is less than the linear buckling load.

To validate the non-linear buckling formulation, Table 3 and 4 shows the comparison of the buckling loads for laminated composite square plates simply supported on all the edges and cantilever conditions, obtained by both linear and non-linear analysis. From the Table 3 and Table 4 it can be said that as the aspect ratio increases the buckling load increases and then decreases for simply supported plates but whereas it remains almost same for the cantilever plates for the same stacking sequence. The buckling load found using the nonlinear analysis is again found lesser than the linear buckling load.

Table-2
Variation of buckling load with aspect ratio for a/h of 100 with different ply lay-ups simply supported on all edges: a/h = 100, E_{11}= 141.0GPa, E_{22} = 9.23GPa, υ_{12}= 0.313, G_{12} = 5.95GPa, G_{23} = 2.96GPa

a/b	Lay ups	Linear Buckling load, N/m	Nonlinear Buckling load
1	0°/90°/0°	77970	76500
	0°/90°/90°/0°	81016	80000
	0°/90°/0°/90°/0°/90°/0°/90°	78537	76500
2	0°/90°/0°	268858	260000
	0°/90°/90°/0°	367000	365500
	0°/90°/0°/90°/0°/90°/0°/90°	334877	332420
3	0°/90°/0°	637851	632000
	0°/90°/90°/0°	821563	815000
	0°/90°/0°/90°/0°/90°/0°/90°	817963	812500

Variation of buckling load with a/h ratio with different ply lay-ups for a cantilever twisted plate with an angle of twist 10° is shown in table-5. From the results it is observed that as the a/h ratio decreases, that is thickness of the plate increases, the non-linear buckling load increases for a particular ply orientation.

Variation of buckling load with aspect ratio for a/h of 250 and angle of twist for a cantilever twisted plate is shown in table-6. From the results it can be said that the buckling value decreases with increase in angle of twist and aspect ratio for the same stacking sequence and side thickness ratio.

The various graphs for nonlinear buckling analysis with different angle of twist which was plotted for Buckling Load Vs Displacement is shown in figure-2. From the graphs it's clear shown that there is a sudden variation of displacement with a very small increase of load which gives the critical buckling load of the problem by nonlinear analysis.

Table-3
Comparison of linear and nonlinear buckling loads for a laminated composite plate[0°/90°/90°/0°] with different aspect ratio simply supported on all edges: a/h = 250 , E_{11}= 141.0GPa, E_{22} = 9.23GPa, υ_{12}= 0.313, G_{12} = 5.95GPa, G_{23} = 2.96GPa

a/b	Buckling load (Linear analysis)N/m	Buckling load (Nonlinear analysis) N/m
1	5211.3	5150
2	23815	23000
3	53598	52000

Table-4
Comparison of linear and nonlinear buckling loads for a laminated composite cantilever plate [0°/90°/90°/0°] with different aspect ratio: a/h = 250 , E_{11}= 141.0GPa, E_{22} = 9.23GPa, υ_{12}= 0.313, G_{12} = 5.95GPa, G_{23} = 2.96GPa

a/b	Buckling load (Linear analysis) N/m	Buckling load (Nonlinear analysis) N/m
1	823.76	786
2	823.28	765
3	823.03	760

Table-5
Variation of buckling load with a/h ratio with different ply lay-ups for a cantilever twisted plate with an angle of twist 10°: a/b = 1 E_{11}= 141.0GPa, E_{22} = 9.23GPa, υ_{12}= 0.313, G_{12} = 5.95GPa, G_{23} = 2.96GPa, Φ = 10°

Lay ups	Nonlinear Buckling load, N/m		
	a/h=250	a/h=200	a/h=150
0°/90°/0°	840	1631	3820
0°/90°/90°/0°	396	1473	3495
0°/90°/90°/0°/0°/90°/90°/0°	535	1036	2467

Table-6
Variation of buckling load with aspect ratio for a/h of 250 and angle of twist for a cantilever twisted plate: a/h = 250, E_{11}= 141.0GPa, E_{22} = 9.23GPa, υ_{12}= 0.313, G_{12} = 5.95GPa, G_{23} = 2.96GPa

a/b	Angle of Twist Φ	Linear Buckling load N/m	Nonlinear Buckling load N/m
1	10°	852.59	840
	20°	735.39	720
	30°	597.70	579
2	10°	763.42	751
	20°	569.01	560
	30°	426.88	420
3	10°	671.11	653.02
	20°	463.94	455
	30°	397.2	390

Conclusion

Instability may occur before a design bifurcation limit is reached. Understanding the large elastic displacement of these types of structures can prevent sudden buckling failures from applied operational and construction loads.

As discussed earlier, the assumptions made in a linear buckling analysis leads to higher values of the buckling load than is obtained from a nonlinear buckling analysis. This can also be observed from the above studies for both flat and twisted composite plates. Hence the above study validates the necessity of a nonlinear buckling analysis, especially for structures whose shape changes drastically during buckling as is the case for thin shell structures.

From the studies on twisted plates, it is observed that as the aspect ratio increases, the buckling load increases for simply supported plates and decreases for cantilever plates but the nonlinear buckling load is less than linear buckling load. It is also observed that the buckling load increases with decrease in side to thickness ratio for the same aspect ratio for laminated twisted composite plate. Also observed from studies that as the angle of twist and aspect ratio increases, buckling load decreases. For a same angle of twist buckling load increases with no. of layers and for symmetric play ups.

References

1. Louis Bauer and Edward L. Reiss, Nonlinear Buckling of Rectangular Plates, *Journal of the Society for Industrial and Applied Mathematics*, **13(3)**, 603–626 **(1965)**

2. David J. Crispino, Richard C. Benson, Stability of twisted orthotropic plates, *International journal of mechanical science*, **28(6)**, 371-379, **(1986)**

3. Eirik Byklum and Jorgen Amdhal, Nonlinear Buckling Analysis and Ultimate Strength Prediction of Stiffened Steel and Aluminium panels, The Second International Conference on Advances in Structural Engineering and Mechanics, Busan, Korea, **(2002)**

4. Judha Purbolaksono and (Ferri) Aliabadi. M.H., Nonlinear buckling formulations and imperfection model for shear deformable plates by the boundary element method, *Journal of Mechanics of Materials and Structures*, **4**, 10, **(2009)**

5. Shaikh Akhlaque-E-Rasul and Rajamohan Ganesan, Non-linear buckling analysis of tapered curved composite plates based on a simplified methodology, *Composites*: Part B, **43**, 797–804, **(2012)**

6. Harvey C. Lee, Buckling Analysis of a Submarine with Hull Imperfections, A Seminar Submitted to the Graduate Faculty of Rensselaer Polytechnic Institute in Partial Fulfillment of the Requirements for the degree of Master of Mechanical Engineering, **(2007)**

7. Sofiyev A.H, Najafov. A.M. and Kuruoglu N, The effect of non-homogeneity on the non-linear buckling behavior of laminated orthotropic conical shells, *Composites*: Part B.,**43**, 1196–1206, **(2012)**

8. Alinia M.M, Soltanieh G. and Amani. M, Inelastic buckling behavior of stocky plates under interactive shear and in-plane bending, *thin-Walled Structures*, **55**, 76-84, **(2012)**

9. Michael J. Lachut and John E. Sader, Buckling of a cantilever plate uniformly loaded in its plane with applications to surface stress and thermal loads , *Journal Of Applied Physics,* 113, **(2013)**

10. Dao Van Dung and Le Kha Hoa, Nonlinear buckling and post-buckling analysis of eccentrically stiffened functionally graded circular cylindrical shells under external pressure, *Thin-Walled Structures*, **63**, 117–124, **(2013)**

11. Dao Huy Bich, Dao Van Dung and Vu Hoai Nam, Nguyen Thi Phuong, Nonlinear static and dynamic buckling analysis of imperfect eccentrically stiffened functionally graded circular cylindrical thin shells under axial compression, *International Journal of Mechanical Sciences*, **74**, 190–200, **(2013)**

12. Yuan. Z and Wang X, Non-linear buckling analysis of inclined circular cylinder-in-cylinder by the discrete singular convolution, *International Journal of Non-Linear Mechanics*, **47**, 699–711, **(2012)**

13. Shariyat M., Non-linear dynamic thermo-mechanical buckling analysis of the imperfect sandwich plates based on a generalized three-dimensional high-order global–local plate theory, *Composite Structures,* **92**, 72–85, **(2012)**

14. Danial Panahandeh-Shahraki, Hamid Reza Mirdamadi and Ali Reza Shahidi, Nonlinear Buckling analysis of laminated composite curved panels constrained by Winkler tensionless foundation, *European Journal of Mechanics A/Solids,* **39**, 120-133, **(2013)**

15. Fazzolari F.A., Banerjee. J.R. and Boscolo M., Buckling of composite plate assemblies using higher order shear deformation theory- analytical approach, *Thin-Walled Structures*, **71**, 18–34, **(2013)**

16. Shruthi Deshpande, Buckling and Post Buckling of Structural Components, University of Texas, **(2010)**

17. Chandrashekhara K., Free vibrations of anisotropic laminated doubly curved shells, *Computers and Structures*, **33(2)**, 435-440, (**1989)**

18. Sahu S.K and Datta P.K, Dynamic stability of laminated composite curved panels with cutouts, *Journal of Engineering Mechanics*, ASCE, **129(11),** 1245-1253, **(2003)**

19. Sandeep Singh, Kamlesh Kulkarni and Ramesh Pandey, Buckling analysis of thin rectangular plates with cutouts subjected to partial edge compression using FEM, *Journal of Engineering, Design and Technology*, **10(1)**, 128-142, **(2012)**

20. Cook R.D., Concepts and applications of finite element analysis, *John Wiley and Sons,* **(1989)**